

# Clumped isotope thermometry of modern and fossil snail shells from the Himalayan-Tibetan Plateau: Implications for paleoclimate and paleoelevation reconstructions

Yang Wang<sup>1,2,†</sup>, Benjamin Passey<sup>3</sup>, Rupsa Roy<sup>1,2</sup>, Tao Deng<sup>4,5</sup>, Shijun Jiang<sup>6</sup>, Chance Hannold<sup>1,2</sup>, Xiaoming Wang<sup>7</sup>, Eric Lochner<sup>8</sup>, and Aradhna Tripathi<sup>9</sup>

<sup>1</sup>Department of Earth, Ocean and Atmospheric Science, Florida State University, Tallahassee, Florida 32306-4100, USA

<sup>2</sup>National High Magnetic Field Laboratory, Tallahassee, Florida 32310, USA

<sup>3</sup>Department of Earth and Environmental Sciences, University of Michigan, Ann Arbor, Michigan 48109, USA

<sup>4</sup>Key Laboratory of Vertebrate Evolution and Human Origins, Institute of Vertebrate Paleontology and Paleoanthropology, Chinese Academy of Sciences, Beijing 100044, P.R. China

<sup>5</sup>College of Earth Sciences, University of Chinese Academy of Sciences, Beijing 100049, P.R. China

<sup>6</sup>Institute of Groundwater and Earth Sciences, Jinan University, Guangzhou 510632, P.R. China

<sup>7</sup>Department of Vertebrate Paleontology, Natural History Museum of Los Angeles County, 900 Exposition Blvd., Los Angeles, California 90007, USA

<sup>8</sup>Department of Physics Condensed Matter and Material Physics User Facility, Florida State University, Tallahassee, Florida 32306, USA

<sup>9</sup>Department of Earth, Planetary, and Space Sciences, Department of Atmospheric and Oceanic Sciences, Institute of the Environment and Sustainability, American Indian Studies Center, Center for Diverse Leadership in Science, University of California, Los Angeles, California 90095, USA

## ABSTRACT

Carbonate clumped isotope thermometry has been applied to fossil mollusk shells from Tibet to reconstruct the paleoclimate and paleoelevation of the region. However, inferred paleoelevation and climatic conditions from this proxy are inconsistent with paleontological evidence. Here, we report new clumped isotope data from both modern and fossil (5–4 Ma) freshwater mollusk shells with the results of X-ray diffraction (XRD) analyses of fossil shells from the Himalayan-Tibetan Plateau. Although all of the fossil shells analyzed in this study appeared pristine based on visual inspection, XRD data reveal that more than half of these apparently “pristine” fossil shells contain trace amounts of calcite. Clumped isotope temperatures derived from the fossil shells display a large range of variation (>22 °C). Among the fossil shells analyzed, those containing traces of calcite have yielded temperatures that are on average ~10 °C lower than those with no detectable calcite from the same strata. These observations sug-


gest that clumped isotope alteration can occur in aragonite shells in low-temperature environments and even in shells with no visible signs of alteration that contain only traces of calcite. The temperatures derived from fossil shells with no detectable calcite are on average 4 °C higher than those derived from modern shells, indicating that southwest Tibet was warmer 4–5 Ma than today. After accounting for temperature change due to global cooling, the difference in clumped isotope temperatures between pristine fossil shells and modern shells suggests that the paleoelevation of the southwestern Tibetan Plateau in the Pliocene was similar to its present-day elevation.

## INTRODUCTION

The uplift of the Himalayan-Tibetan Plateau is thought to have been a major driver of regional and global climate change during the Cenozoic (An et al., 2001; Ruddiman et al., 1997). However, the timing of the Tibetan uplift and its effects on Earth's climate and biosphere remain a matter of much debate and speculation (An et al., 2001; Botsyun et al., 2019; DeCelles et al., 2007; Deng and Ding, 2015; Deng et al., 2019; Molnar et al., 2006; Quade et al., 2011; Saylor et al., 2016; Wang et al., 2006; Wang et al., 2012). Lo-

cal and regional climate changes could be caused by tectonic change and/or global climate change. Teasing apart these effects is difficult without reliable knowledge of paleotemperatures and paleoelevations.

Paleoclimatic reconstructions using geochemical and biological proxies from the Tibetan plateau have often yielded inconsistent results. For example, reconstruction of paleo-meteoric water  $\delta^{18}\text{O}$  and paleotemperature estimates from isotopes in fossil shells from the Zanda Basin in southwestern Tibet suggest that the area was arid and cold and had a 1–1.5 km higher elevation during the late Miocene and Pliocene than today (Huntington et al., 2015; Murphy et al., 2009). In contrast, pollen evidence (Han et al., 2012; Li and Zhou, 2002; Zhu et al., 2007) and the discovery of fossil rhino Dicerorhininae (Meng et al., 2004) in the same basin suggest a warmer and wetter climate in the late Miocene–Pliocene than today. Deng et al. (2011, 2012) argued that the Zanda Basin had reached high elevations similar to that of today and that local climate had become cold by the mid-Pliocene based primarily on occurrence in the basin of the most primitive woolly rhinoceroses (*Coelodonta thibetana*) and three-toed horses (*Hipparion zandaense*) that were adapted to living in cold climates above the tree line. This view was supported by tooth

Yang Wang  <http://orcid.org/0000-0002-8232-3289>

<sup>†</sup>ywang@magnet.fsu.edu.

enamel stable isotope data from a diverse group of fossil herbivores found in the basin that suggest little or no warm climate C<sub>4</sub> grasses in local habitats (Deng et al., 2011; 2012; Wang et al., 2013b; 2015). Mammalian tooth enamel isotope data also suggest that the Zanda Basin was wetter in the mid-Pliocene than it is today (Wang et al., 2013b). Reliable paleotemperature reconstructions can help to resolve the discrepancies between these different types of climatic indicators.

Fossil mollusk shells, which are made of carbonate, are abundant in ancient lake deposits on the Tibetan Plateau and are valuable archives of paleoclimate and paleoelevation (Saylor et al., 2009; Wang et al., 2008). The oxygen isotope compositions ( $\delta^{18}\text{O}$ ) of shell carbonates contain information about water temperature and water  $\delta^{18}\text{O}$  values. However, it is difficult to reconstruct paleotemperature using the conventional oxygen isotope thermometer (e.g., Kim et al., 2007) because it requires an assumption about (or independent knowledge of) the  $\delta^{18}\text{O}$  of the water from which a mineral was formed to determine the temperature or vice versa. The recently established carbonate clumped isotope thermometer (Ghosh et al., 2006a) has great potential to provide a reliable tool for reconstructing temperatures, hydrological conditions, and elevations of ancient environments (Eiler, 2011; Ghosh et al., 2006b; Huntington et al., 2015; Quade et al., 2013). The method is based on the thermodynamic preference of heavy isotopes of carbon (<sup>13</sup>C) and oxygen (<sup>18</sup>O) to “clump” with each other (<sup>13</sup>C-<sup>18</sup>O) in carbonate minerals (Ghosh et al., 2006a). The “clumping” is quantified by the parameter  $\Delta_{47}$ , which is a measure of the abundance of <sup>13</sup>C-<sup>18</sup>O bonds in the carbonate lattice relative to that expected at a random distribution of isotopes among all isotopologues (Ghosh et al., 2006a). The  $\Delta_{47}$  value is inversely correlated with the temperature of mineral formation independent of the  $\delta^{18}\text{O}$  values of the water from which the carbonates form (Ghosh et al., 2006a). This gives the method a significant advantage over the conventional carbonate oxygen isotope thermometer because it allows the temperature of mineral formation to be calculated directly from the  $\Delta_{47}$  value of the carbonate.

In this study, we measured the clumped isotope compositions of Pliocene fossil freshwater shells as well as modern *Radix* snail shells from the Himalayan-Tibetan Plateau. The new data, in conjunction with X-ray diffraction analysis results and previously published clumped isotope data, were used to evaluate the clumped isotope thermometry of freshwater snail shells from the high plateau and to improve the accuracy of the interpretation of clumped isotope data from fossil freshwater shells in terms of paleoclimate and paleoelevation. Our results have important

implications for paleoclimate and paleoelevation reconstructions using clumped isotope data from aragonite fossil shells.

## MATERIALS AND STUDY SITES

### Modern Shells

Modern freshwater mollusk shells were collected, along with water samples, from seven different lakes on the Himalayan-Tibetan Plateau for this study, including Lake Manasarovar, Yamdrok Yumco, Nam Cuo, Seling Cuo, Cuoner, Yaxi Cuo, and Qia-gui Cuo (Fig. 1). Most of our modern samples were collected in August of 2013 except for two shell samples (TB07S-1 and TB07S-1a) that were collected from Lake Manasarovar in August of 2007. Samples from Nam Cuo and Yamdrok Yumco were collected live from shallow (or melt-water) ponds adjacent to the lakes in late August of 2013, and the rest of the samples were dead shells collected along the lakeshore areas. All of the modern shells are intact and belong to the genus *Radix*.

### Fossil Shells

Fossil freshwater snail shells analyzed in this study were collected from the late Cenozoic lacustrine sediments on the Himalayan-Tibetan Plateau. The majority of our fossil shell samples were collected from the Pliocene strata in the Zanda Basin in southwestern Tibet with the exception of two Pliocene samples from the Kunlun Pass Basin and two Pleistocene shells from

Quan-ji in the Qaidam Basin on the northern Tibetan Plateau (Fig. 1). All of our fossil shell samples are intact or nearly intact whole shells except for the samples from the Kunlun Pass Basin that are mixtures of shell fragments recovered from screen wash for small mammal fossils. In addition, a few shell samples of unidentified species from the Miocene lacustrine deposits in the region were also included in this study.

The Zanda Basin (~31–32°N, ~79–80°E), which is sometimes spelled as Zhada (or Zada) and was also known as Tsaparang in old western literature (Wang et al., 2020), is located in the northern foothills of the western Himalaya. It is the largest Neogene sedimentary basin on the southwestern Tibetan Plateau (Saylor et al., 2009; Saylor et al., 2016; Wang et al., 2013a). The present-day elevation of the basin is ~3800–4500 m above sea level (a.s.l.) with a mean annual air temperature (MAAT) around 0–3 °C and annual precipitation (AP) of ~200 mm (Wang et al., 2013b). The basin contains late Miocene-Pleistocene lacustrine and fluvial/alluvial sediments that span continuously from ca. 9 Ma to <1 Ma (Saylor et al., 2009; Wang et al., 2013a). Sediments in the Zanda Basin contain abundant gastropod, fish, and mammalian fossils, and the chronology of the sedimentary sequence has been established through magnetostratigraphic and biostratigraphic studies (Saylor et al., 2009; Wang et al., 2013a). The Zanda Basin fill is undeformed and was deposited over an angular unconformity on top of Tethyan basement strata with substantial paleo-topology. Freshwater snails, such as *Radix*, are ubiquitous in all

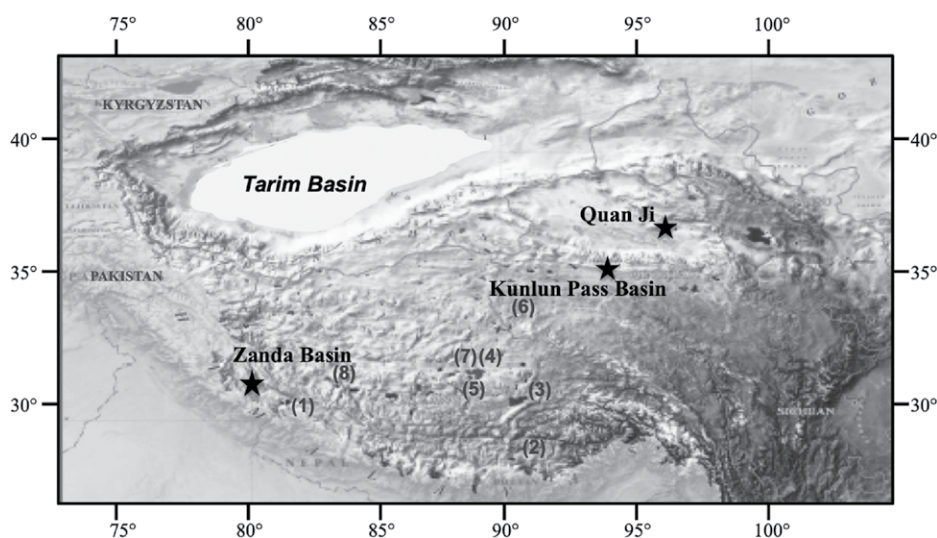


**Figure 1.** Our sample locations are shown in this aerial image of the Himalayan-Tibetan Plateau (<https://image.baidu.com>). Stars mark the fossil sites, and numbers indicate the modern lakes where modern shells were analyzed: (1) Lake Manasarovar; (2) Yamdrok Yumco; (3) Nam Cuo; (4) Seling Cuo; (5) Cuoner; (6) Yaxi Cuo; (7) Qia-gui Cuo; and (8) Ngangla Ring Cuo, where daily lake water temperature data are available (Huntington et al., 2015).

fine-grained sediments and are likely fully aquatic. Saylor et al. (2010) show that sedimentary deposits in the Zanda Formation occur in two types of cycles (type A and B) that mark periods of lake expansion and contraction. The lower part of the Zanda Formation is dominated by the “type A cycle” that typically consists of a 1–10-m-thick unit of fluvial or alluvial fan sandstone or conglomerate with an erosional base, no grain-size trend, and a capping, upward fining sandstone bed (Saylor et al., 2010). The middle and upper part of the Zanda Formation, from which our fossil shells were collected, is characterized by the “type B cycle” (Saylor et al., 2010). A typical “type B cycle” consists of an upward-coarsening succession of fossil-rich claystone and siltstone, and wave-worked sandstone and conglomerate, representing progradational lacustrine sequence and deltaic or lake margin deposits (Saylor et al., 2009; 2010). Because our snail samples were collected from the fine-grained lacustrine sediments (claystone and siltstone) rather than the coarser fluvial/alluvial sediments, it is not very likely that they were transported by rivers from higher elevations into the lake. Instead, these fossil freshwater snails (associated with the fine-grained lake sediments) most likely lived in the paleo-Zanda lake throughout their lifetimes. The undisturbed flat-lying beds in the basin are less than 900 m in total thickness and therefore have not been subjected to high-temperature alteration nor solid-state reordering due to burial temperatures approaching the proposed  $\sim 100$  °C limit for preservation of original  $\Delta_{47}$  values in calcite (Henkes et al., 2014). Our fossil shells represent two extinct species: *Radix zandaensis* (in the family Physidae) and *Veletinopsis spiralis* Yu (belonging to the family Lymnaeidae). Han et al. (2012) suggest that both species lived in a shallow littoral lake environment in a warmer and wetter climate than today based on comparison with existing species and pollen evidence.

The Kunlun Pass Basin ( $\sim 35^{\circ}35' - 35^{\circ}42'N$ ,  $\sim 94^{\circ}00' - 94^{\circ}20'E$ ) is located in the Kunlun Pass area of the East Kunlun Mountains on the northern Tibetan Plateau. The elevation of the basin is  $\sim 4600 - 5300$  m a.s.l. The peaks of the East Kunlun Mountains exceed 6 km a.s.l. The MAAT in the area is well below freezing, and the estimated AP is  $\sim 276$  mm (Wang et al., 2008). The Kunlun Pass Basin is a pull-apart basin bounded by major faults, and the basin is filled with Pliocene and Quaternary alluvial, lacustrine, and glacial deposits unconformably overlying Triassic metamorphic basement rocks (Song et al., 2005). Our fossils were collected from the laminated, organic-rich lacustrine siltstones of the lower Qiangtang Formation that contain abundant plant remains and ostracod and gastropod shells (Wang et al., 2008). The ages of the fossils were

previously estimated to be 2.0–2.5 Ma (Wang et al., 2008). A recent study of small mammals suggests that they should be of Pliocene age, around 3.6–4.2 Ma (Li et al., 2014).

The Qaidam Basin ( $36 - 39^{\circ}N$ ,  $90 - 98^{\circ}E$ ) is the largest intermontane basin on the northern Tibetan Plateau and has an average elevation of  $\sim 3$  km a.s.l. The MAAT is  $\sim 4 - 5$  °C, and the AP is  $< 100$  mm (Zhang et al., 2012). Cenozoic deposits in the Qaidam Basin are primarily fluvial, alluvial, or lacustrine sedimentary rocks and unconsolidated sediments. Abundant mammalian and aquatic fossils have been found from the late Cenozoic strata in the eastern part of the basin (Wang et al., 2015; Zhang et al., 2012). Shell samples analyzed in this study were from the Quan Ji locality in the eastern central Qaidam Basin (Fig. 1) and were identified as *Radix* sp. The sedimentary sequence at Quan Ji (with a total thickness of  $\sim 50$  m) consists primarily of fine-grained lacustrine sediments intercalated with aeolian and fluvial sand and is thought to have been deposited at or near the margin of a large freshwater lake that once existed in the Qaidam Basin in the middle Pleistocene (Mischke et al., 2010). Based on infrared stimulated luminescence dating of feldspars in sand samples and  $^{230}Th/U$  dates on biogenic carbonates, Mischke et al. (2010) suggested that the sediments at Quan Ji accumulated between 120 ka and 400 ka in the Pleistocene.

## METHODS

Based on visual inspection, well-preserved fossil shells were selected for X-ray diffraction (XRD) analyses. The selected fossil shells were cleaned in a weak HCl solution ( $< 1\%$ ) in an ultrasonic bath for  $\sim 5 - 10$  min, rinsed with distilled water (DI), and air-dried. The cleaned shells were then ground into fine powder for XRD analyses, and a subset of the shell samples were selected for clumped isotope analyses. Modern snail shells were soaked in 30%  $H_2O_2$  for an hour or longer to remove organic matter from the shells and then rinsed with DI water and air dried. Cleaned shells were ground into powder for clumped isotope analyses. Each modern shell sample consists of a single shell ( $\geq 1.2$  mm in length) except for two samples (Yam2s-4 and Nam1s-1) that are each a mixture of three small shells ( $\sim 0.5$  mm). For clumped isotope analyses, one large modern *Radix* shell, YXC-5 (24 mm long) from Ya-xi-cuo, was sectioned using a slow-speed drill along the growth direction into four subsamples representing different stages of the snail's life cycle.

For XRD analysis, the sample was dusted through a 200 mesh sieve onto zero-background holders for measurements on a Siemens D500

diffractometer in the Condensed Matter and Material Physics (CMMP) User Facility at Florida State University (FSU). The data span  $25 - 31^{\circ}$  at  $0.02^{\circ}$  steps and a  $0.5^{\circ}/min$  scan rate. The data were smoothed, and then the powder diffraction file (PDF) standards for calcite and aragonite were used to refine the aragonite peaks simultaneously with the calcite peak positions. The percentages of calcite and aragonite in a sample were determined based on the strongest lines (peaks) of the phases present. Each of those strongest lines has a reference intensity ratio (RIR) that is the diffracted intensity of the strongest line of that phase to that of an intensity standard: corundum ( $Al_2O_3$ ). For calcite, the RIR is 2.0; for aragonite, it is 1.0. The peak heights were divided by the RIRs and normalized to 100% to obtain the weight percentages. The detection threshold is 0.3%–0.4% as the peak fitting always yields a peak intensity even when there is no obvious peak present. Thus, samples with  $< 0.4\%$  calcite are considered pristine (or pure aragonite).

For clumped isotope analysis, the samples and carbonate standards ( $\sim 8$  mg each) were reacted with anhydrous  $H_3PO_4$  at 90 °C, and the resultant  $CO_2$  was purified cryogenically and by passage through a Porapak-Q gas chromatography (GC) column held at  $-20$  °C. Mass 44–49 isotopologue ratios were measured using a Thermo MAT 253 mass spectrometer, and the data were reduced using the scheme detailed in Huntington et al. (2009) and Henkes et al. (2013). An acid temperature correction factor of  $+0.081\%$  was applied to all data to normalize values to 25 °C reactions (Ghosh et al., 2006a; Passey et al., 2010). Two carbonate standards (NBS-19 and 102-GC-AZ01) were analyzed for every five or six samples. Aliquots of  $CO_2$  gases driven to isotopologue equilibrium at 1000 °C and 30 °C were also analyzed every two or three days. All new clumped isotope ( $\Delta_{47}$ ) data are reported relative to the Absolute Reference Frame (ARF) (Dennis et al., 2011). The data obtained previously are reported relative to the old “heated gas” or “Ghosh” scale (e.g., Ghosh et al., 2006a; Huntington et al., 2009) since they were analyzed prior to conception of the ARF (Dennis et al., 2011). The stable C and O isotope data are reported in standard notation as  $\delta^{13}C$  and  $\delta^{18}O$  values in reference to the international standard Vienna Pee Dee Belemnite (VPDB). The analytical precision based on repeated analyses of carbonate standards (processed with the samples) is  $\pm 0.017$  (one standard deviation from the mean,  $1\sigma$ ) for 102-GC-AZ01 and  $\pm 0.016$  ( $1\sigma$ ) for NBS-19, equivalent to an uncertainty in calculated temperature of  $\pm 6$  °C. The majority of the samples were analyzed using a Thermo MAT 253 mass spectrometer coupled

to a custom-built, automated acid reaction and gas purification line in the Department of Earth and Planetary Science at John Hopkins University (JHU). Only eight samples were analyzed previously, using a nearly identical system, at the California Institute of Technology (Caltech), including the four shells from the mid-Pliocene strata in Zanda Basin reported in Wang et al. (2013b). The calibrations used for calculating temperatures are generated using these same systems. To ensure that our data are comparable to the previously published data from Tibet (Wang et al., 2013b; Huntington et al., 2015), temperatures were calculated from the  $\Delta_{47}$  values using the mollusk-specific calibration of Henkes et al. (2013) and also the “Aragonitic bivalve mollusks” calibration of Eagle et al. (2013), which are referred to as the “Henkes calibration” and “Eagle calibration,” respectively, hereafter. All data are on the Gouffanti parameter set, as are the calibrations that were used to calculate temperatures. To verify if results from different labs are comparable, we re-analyzed some of the fossils in the Isotopologue Paleosciences Laboratory at the University of Michigan (UM) and additional modern samples from two of the study lakes in the lab at the University of Cali-

fornia at Los Angeles (UCLA). In addition, the isotope ratios from these analyses are calculated using the Brand parameter set, as is the temperature calibration used (e.g., Petersen et al., 2019). About 60% of our samples (28 out of 47 samples) were analyzed in replicates.

Water samples were analyzed using equilibration methods (Thermo Finnigan Operating Manual); 500 micro-liter ( $\mu\text{L}$ ) of water was pipetted into an open vial containing a platinum catalyst rod. The vial was then sealed with a new septum. Vials containing water samples and standards were then flushed with He containing either 2%  $\text{H}_2$  (for  $\delta\text{D}$  analyses) or 0.3%  $\text{CO}_2$  (for  $\delta^{18}\text{O}$  analyses) and allowed to equilibrate isotopically for 24 h at 25 °C. Headspace gas was then introduced into a Finnigan MAT DELTA plus XP Stable Isotope Ratio Mass Spectrometer for isotope analysis at FSU. Results are reported in standard delta ( $\delta$ ) notation as  $\delta^{18}\text{O}$  values in reference to the international water standard Vienna Standard Mean Ocean Water (VSMOW). The analytical precision (based on repeated analyses of VSMOW and several other lab standards processed with each batch of samples) is  $\pm 0.1\text{‰}$  or better for  $\delta^{18}\text{O}$ . The  $\delta\text{D}$  data (not discussed in this paper) will be reported elsewhere.

## RESULTS

We measured the clumped and stable isotope compositions of 31 modern mollusk shell samples from seven Tibetan lakes (Supplemental Table S1<sup>1</sup>). We also performed XRD analysis on 33 fossil mollusk shells from the Tibetan Plateau (Table S2; see footnote 1) and analyzed 16 of these fossil shells for clumped and stable isotopes (Table S3; see footnote 1). The results are summarized in Figures 2–6.

There is little or no difference between temperature values calculated using data generated previously on the Gouffanti parameter set and the older mollusk-specific calibrations or the Brand parameter set and a recent calibration that represents a synthesis of data from multiple groups and includes results for mollusks (Petersen et al., 2019) (Table S4; see footnote 1). Results from different labs are generally comparable. As shown in Figure S1 and Table S3 (see footnote 1),

<sup>1</sup>Supplemental Material. Supplementary figures and tables. Please visit <https://doi.org/10.1130/GSAB.S.12996533> to access the supplemental material, and contact [editing@geosociety.org](mailto:editing@geosociety.org) with any questions.

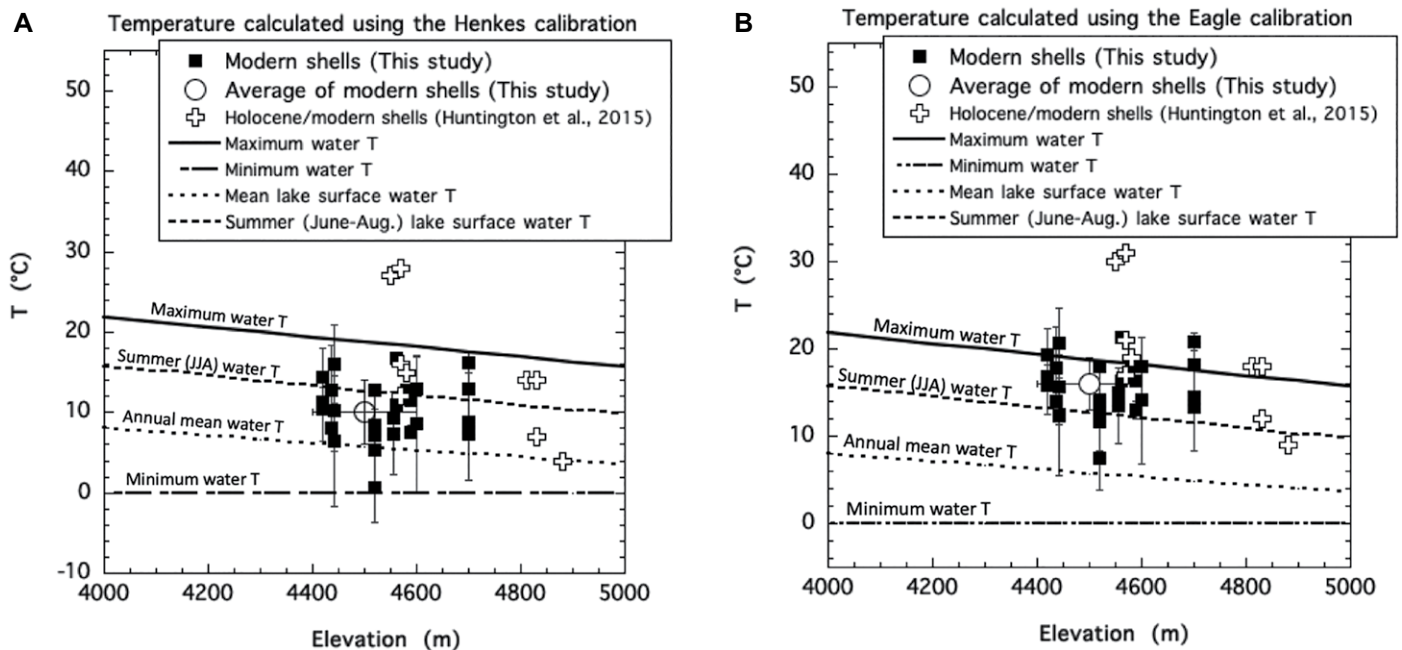


**Figure 2.** Comparison of clumped isotope temperatures of modern *Radix* shells from Tibetan Lakes with previously published data from Holocene and modern shells is shown (Huntington et al., 2015). (A) Temperatures calculated using the mollusk-specific  $\Delta_{47}$  temperature calibration of Henkes et al. (2013), and (B) temperatures calculated using the “Aragonitic bivalve mollusks” calibration of Eagle et al. (2013). Also shown are the estimated modern maximum, minimum, mean annual, and summer (June–August) lake surface water temperatures at the sampling sites. The maximum lake surface water temperatures were estimated using the equation ( $T = -0.0061 \times \text{elevation} + 46.159$ ) given in Huntington et al. (2015). Mean annual surface water temperatures and summer lake water temperatures were calculated using the relationships between mean annual air temperature (MAAT) and lake water temperatures (Hren and Sheldon, 2012), and the MAAT for each sample locality was calculated using the relationship between MAAT and elevation for the region (Quade et al., 2011). Error bars indicate 1 standard deviation from the mean value.

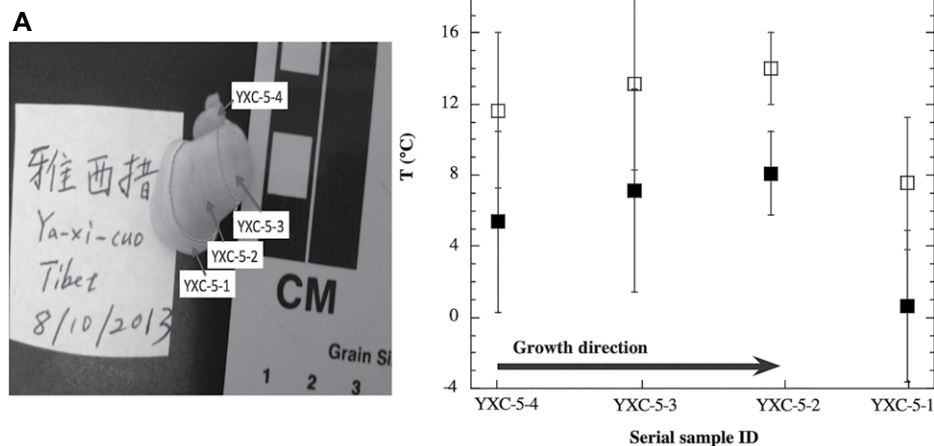


**Figure 3.** Clumped isotope temperatures of time-serial sub-samples from a modern freshwater mollusk shell (YXC-5) from Tibetan Lake Ya-xi-cuo show that the snail was born probably in the early spring, lived throughout the warm season, and died in the winter or following spring. Error bars indicate 1 standard deviation from the mean of replicate/triplicate analyses of the same sample.

re-analyses of selected fossils that were analyzed previously at Caltech and JHU at UM yielded the same  $\delta^{18}\text{O}$  and  $\delta^{13}\text{C}$  values and similar  $\Delta_{47}$ -temperatures for the same samples. Analyses at UCLA Lab of additional modern samples from two of the lakes also yielded results very similar to those obtained from the JHU Lab for the same lakes except for two samples (T16-05G-3 and T16-05G-4) from Lake Manasarovar (Fig. S1D;

Table S1). These two samples were excluded from further discussion because their replicated analyses yielded not only very large temperature ranges (from  $-1.3\text{ }^{\circ}\text{C}$  to  $26\text{ }^{\circ}\text{C}$  for T16-05G-3 and from  $13\text{ }^{\circ}\text{C}$  to  $30\text{ }^{\circ}\text{C}$  for T16-05G-4) that are much larger than the reported analytical uncertainty but also unreasonably high temperatures that greatly exceed the maximum lake water temperature for the high-elevation lake.

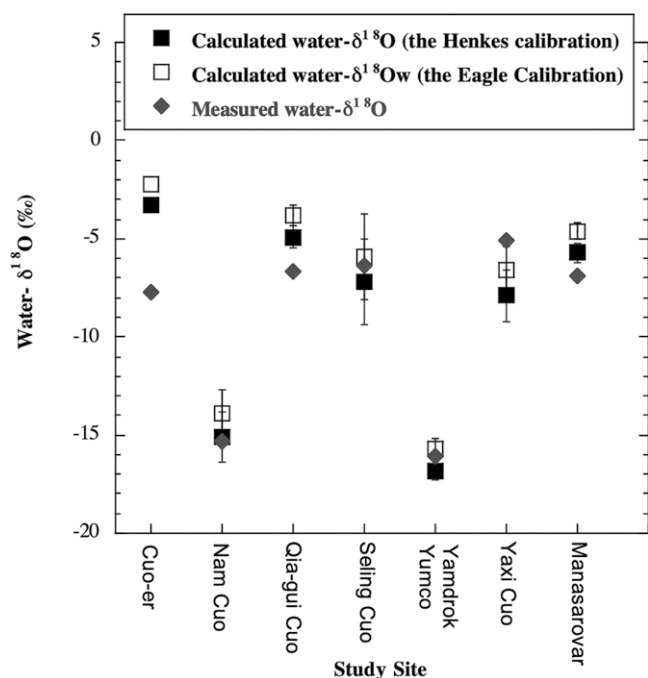


**Figure 4.** Comparison shows calculated water  $\delta^{18}\text{O}$  values with the measured  $\delta^{18}\text{O}$  values of water samples from the lake sites. Error bars indicate 1 standard deviation from the mean of all samples analyzed from the sites.

**DISCUSSION**

**Clumped Isotope Signatures of Modern Shells from Tibetan Lakes**

Temperatures calculated from the  $\Delta_{47}$  values of our modern *Radix* shells from various lakes across the Himalayan-Tibetan Plateau range from  $1\text{ }^{\circ}\text{C}$  to  $17\text{ }^{\circ}\text{C}$ , with a mean of  $10 \pm 4\text{ }^{\circ}\text{C}$  ( $n = 29$ ), using the Henkes calibration (Fig. 2A). In comparison, the temperatures calculated using the Eagle calibration vary from  $8\text{ }^{\circ}\text{C}$  to  $21\text{ }^{\circ}\text{C}$ , averaging  $16 \pm 3\text{ }^{\circ}\text{C}$  ( $n = 29$ ) (Fig. 2B). The clumped isotope temperatures derived from the Eagle calibration are on average  $6\text{ }^{\circ}\text{C}$  higher than those from the Henkes calibration, and the difference between the two becomes larger (up to  $7\text{ }^{\circ}\text{C}$ ) at low temperatures and smaller at or near the high-temperature end of the temperature range observed in the shells (Figs. 2, 3, and 5B).

There are no long-term temperature records for the Tibetan lakes where our samples were collected. The only available lake water temperature record in the region is from Ngangla Ring Cuo—a large closed basin lake (Fig. 1) in the central Tibetan Plateau (Huntington et al., 2015). Hourly surface water temperatures recorded continuously throughout one year using a temperature logger at Ngangla Ring Cuo varied from  $0\text{ }^{\circ}\text{C}$  in the winter to a maximum of  $17\text{ }^{\circ}\text{C}$  on the warmest day in the summer with a mean annual water temperature (MAWT) of  $7\text{ }^{\circ}\text{C}$  and an average summer water temperature of  $12.8\text{ }^{\circ}\text{C}$  (Huntington et al., 2015). Based on analyses of temperature records from various lakes across the globe, Hren and Sheldon (2012) show that lake surface water temperatures are strongly correlated with MAAT independent of lake size. Using the empirical relationships between lake water temperatures and MAAT given in Hren and Sheldon (2012) and the MAAT-elevation relation for the region (Quade et al., 2011), we predicted surface water temperatures for our study lakes (Fig. 2). The predicted MAWT and summer water temperature for Ngangla Ring Cuo ( $\sim 4700\text{ m a.s.l.}$ ) are  $5\text{ }^{\circ}\text{C}$  and  $11\text{ }^{\circ}\text{C}$ , respectively, very similar to those measured in situ (Huntington et al., 2015). This gives confidence that the predicted lake water temperatures (based on the previously published empirical relations) provide reasonable estimates of surface water temperatures of our study lakes. The clumped isotope temperatures of the modern shells calculated using the Henkes calibration fall within the range of water temperature variations observed at Ngangla Ring Cuo and also within the predicted surface water temperature variation range at each sample site (Fig. 2A). However, some of the temperatures calculated using the Eagle calibration lie outside the observed and predicted variation range of

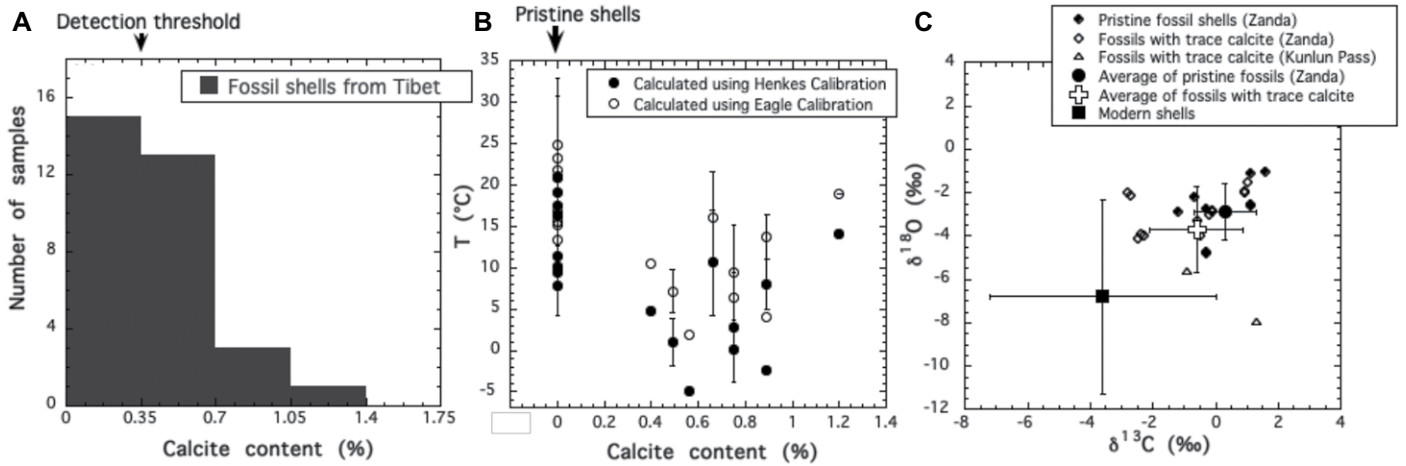


**Figure 5.** (A) X-ray diffraction analysis results of fossil aragonitic mollusk shells with no visible signs of alteration from the Tibetan Plateau are shown. (B) Plot of clumped isotope temperatures versus calcite content in Pliocene aragonite fossil shells; shells with calcite content below the detection threshold (<0.4%) are considered to be pure aragonite or pristine. (C) Plot of  $\delta^{18}\text{O}$  versus  $\delta^{13}\text{C}$  values of fossil and modern shells. The error bars in (B) indicate 1 standard deviation from the mean of replicated analyses of a sample. The error bars in (C) indicate 1 standard deviation from the mean of all samples in a given group.

lake water temperatures (Fig. 2B). The average temperature derived from our modern shells using the Henkes calibration is similar but slightly higher than the MAWT (Fig. 2A). In compari-

son, the average temperature derived from our modern shells using the Eagle calibration is very similar to (but slightly lower than) the maximum water temperature (Fig. 2B).

Huntington et al. (2015) reported clumped isotope data from nine early Holocene and modern lymnaeid shell samples collected from diverse habitats (interdune pools, creeks,

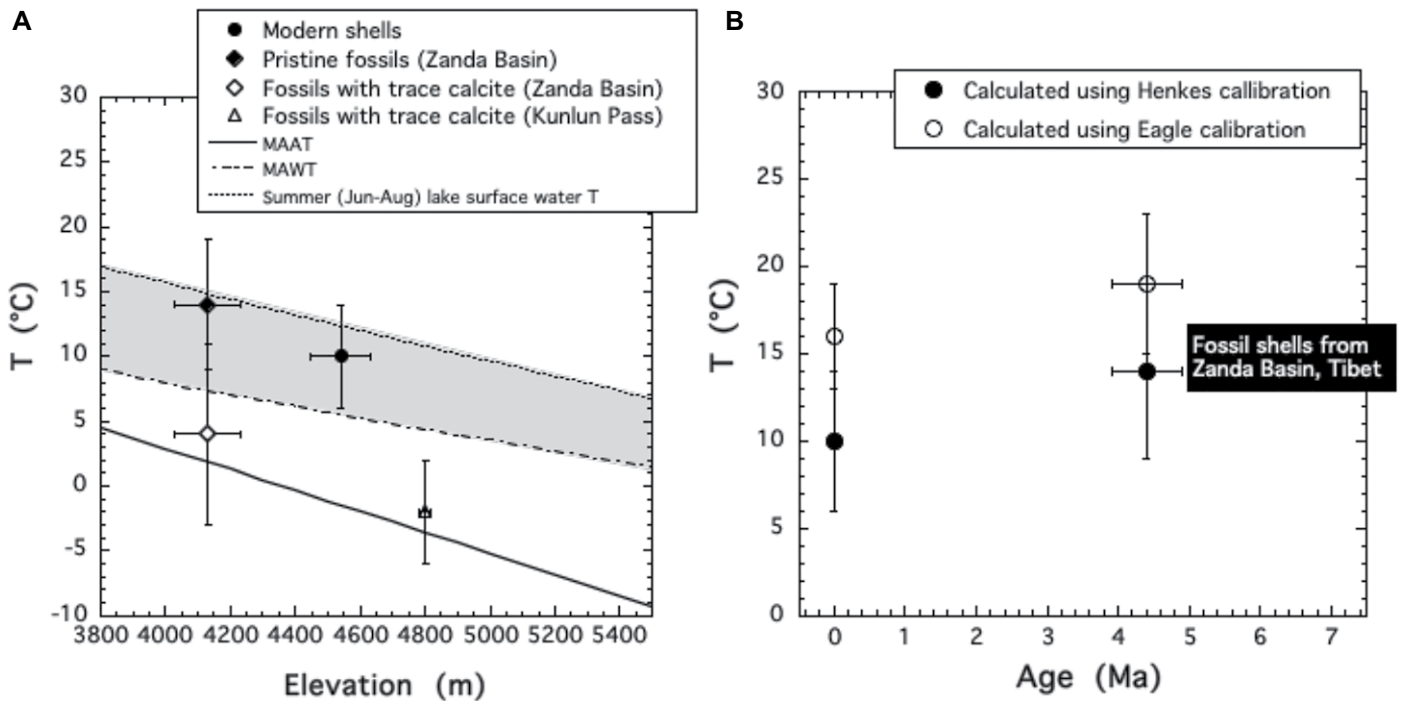


**Figure 6.** (A) Comparisons are shown of clumped isotope temperatures of modern and fossil freshwater mollusk shells from the Tibetan Plateau with estimated mean annual air temperature (MAAT), mean annual lake surface water temperature (MAWT), and summer (June–August) lake surface water temperature at the present-day elevation of the sampling sites; and (B) comparison of modern shells and pristine fossil shells from Zanda Basin, southwestern Tibet. The MAAT for each sample locality was calculated using the relationship between MAAT and elevation for the region (Quade et al., 2011). The MAWT and summer lake water temperatures were calculated using the relationships between MAAT and lake water temperatures (Hren and Sheldon, 2012). Error bars indicate 1 standard deviation from the mean value.

wetlands, paleo-shorelines, and lakes) on the central Tibetan Plateau. As shown in Figure 2, the temperatures calculated from the  $\Delta_{47}$  values of their early Holocene/modern shells varied from 4 °C to 28 °C, averaging  $15 \pm 8$  °C, using the Henkes calibration, and from 9 °C to 31 °C, with an average of  $20 \pm 7$  °C, using the Eagle calibration (Huntington et al., 2015). Two of their shells (DT10-9-3 and Zhongba10-6b) yielded unreasonably high temperatures of 30 °C and 31 °C using the Eagle calibration (or, 27 °C and 28 °C using the Henke calibration) (Fig. 2; Table S1). Excluding these two samples, the  $\Delta_{47}$ -derived temperatures for the remainder of their early Holocene/modern shells are  $12 \pm 5$  °C ( $n = 7$ ) using the Henkes calibration or  $16 \pm 4$  °C ( $n = 7$ ) using the Eagle calibration, which is very similar to the temperatures derived from the  $\Delta_{47}$  values of our modern *Radix* shells (Fig. 2; Table S1).

*Radix* snails are known to prefer quiet environments such as shallow littoral zones of lakes, ponds, or slow-moving streams; they usually have a life span of about one year and can live through the winter by migrating into deeper water and staying active under the ice cover in frozen lakes (Økland, 1990; Taft et al., 2012). Sclerochronological  $\delta^{18}\text{O}$  analyses of *Radix* shells from Tibetan lakes have shown that *Radix* shells faithfully record seasonal variations in the ambient water conditions (Taft et al., 2012; Roy et al., 2019). Based on detailed analyses of intra-shell  $\delta^{18}\text{O}$  patterns and seasonal variations in the  $\delta^{18}\text{O}$  and temperature of lake water along a climatic transect, Roy et al. (2019) suggest that *Radix* is able to reproduce throughout the year in regions where water temperatures do not fall below 10 °C but could only reproduce in the summer or late spring under extreme climatic conditions on the present-day Tibetan Plateau (Roy et al., 2019). Roy et al. (2019) also show that the average growth temperatures (calculated using the conventional aragonite-water  $\delta^{18}\text{O}$  thermometer) of large *Radix* shells ( $\geq 1.4$  cm) closely approximate the MAWT. Smaller *Radix* shells ( $< 1.4$  cm), on the other hand, represent less than 1 year of growth and can yield temperatures that may be higher or lower than the MAWT (depending on the times of their shell formation) but are within the observed variation range of lake water temperature (Roy et al., 2019). Assuming that the Eagle calibration is most suitable for the freshwater snail shells, the clumped isotope temperatures of modern shells from the Tibetan lakes would suggest that the *Radix* and other lymnaeid snails could only grow at the warmest times of a year when water temperatures are close to or exceed the average summer water temperature (Fig. 2B). Alternatively, if the Henkes

calibration is assumed to be the most appropriate for the freshwater shells, the temperatures calculated from the  $\Delta_{47}$  values of our modern *Radix* shells from Tibetan lakes would suggest that these snails could grow throughout a year recording seasonal variations in lake water temperature. This is consistent with the known life cycle of these organisms and the detailed stable isotope profiles of individual *Radix* shells from the Tibetan Plateau (Roy et al., 2019; Taft et al., 2013). Thus, the Henkes calibration appears to be more suitable for the freshwater mollusk shells examined in this study (Fig. 2).

The average clumped isotope temperature of our modern *Radix* shells calculated using the Henkes calibration ( $10 \pm 4$  °C) falls in between the predicted MAWT and the average summer (June–August) temperature (Figs. 2A). Although the difference between the average  $\Delta_{47}$ -derived temperature and the predicted MAWT is within the analytical uncertainty ( $\pm 6$  °C), this may suggest a small bias in growth toward the warm season, which is consistent with detailed stable isotope profiles of individual shells (Roy et al., 2019; Taft et al., 2013) and also supported by our clumped isotope data from sub-samples of an individual shell. As shown in Figure 3A, samples YXC-5-1, YXC-5-2, YXC-5-3, and YXC-5-4 are sub-samples collected along the growth direction of a large *Radix* shell (24 mm long) with YXC-5-4 representing earliest growth and YXC-5-1 the latest growth before death. The clumped isotope temperatures of these sub-samples range from  $1 \pm 4$  °C to  $8 \pm 2$  °C using the Henkes calibration and from  $8 \pm 4$  °C to  $14 \pm 2$  °C using the Eagle calibration (Fig. 3B). Despite the very coarse sampling resolution (as sample size required for clumped isotope analysis is  $\sim 100$  times larger than that for traditional stable isotope analysis), the  $\Delta_{47}$ -derived temperatures of these sub-samples display significant variations, which reflects seasonal variations in lake environment (Fig. 3B).

From the clumped isotope temperatures and the  $\delta^{18}\text{O}$  values of the shells, we calculated the water  $\delta^{18}\text{O}$  values using the aragonite-water oxygen isotope fractionation equation of Kim et al. (2007) (Fig. 4). The calculated water  $\delta^{18}\text{O}$  values range from  $-2\text{‰}$  to  $-17\text{‰}$  (Fig. 4). These values are very similar to the measured  $\delta^{18}\text{O}$  values of the water samples collected from the shell sampling localities, except for two lakes (i.e., Cuo-er and Qia-gui Cuo) (Fig. 4). The discrepancies are expected as the  $\delta^{18}\text{O}$  value of lake water may vary significantly with time and location within a lake on the Tibetan Plateau (Roy et al., 2019), and different lakes can have different water  $\delta^{18}\text{O}$  values (Fig. 4) depending on many local factors such as water residence time, evaporation/precipitation ratio, distance from river/stream inlets, etc.

## Mineralogy and Clumped Isotope Signatures of Fossil Shells

Fossil shells are a valuable archive of paleoclimate provided that their original isotopic signatures have not been altered in postmortem environments. The shells of freshwater mollusks are made of the carbonate mineral aragonite. It is well known that aragonite is thermodynamically less stable than calcite in surface environments and is prone to recrystallization to the more stable calcite (Sharp, 2007). Thus, unaltered fossil shells should be composed only of aragonite, and detection of calcite in aragonite shells is a good indication of diagenetic alteration. The mineralogical integrity of a fossil shell can be examined using XRD analysis.

In this study, we selected 25 Pliocene, two Pleistocene, and six Miocene fossil freshwater shells that appeared to be “pristine” based on visual inspection for XRD analyses, including the four shells whose clumped isotope temperatures were previously reported (Wang et al., 2013b). The XRD analysis results show that many of the samples had calcite contents below the detection threshold ( $< 0.4\%$ ) and can be considered to be pure aragonite (Table S2). However, more than half of these visually “pristine” fossil shells contain detectable amounts of calcite (Fig. 5A; Table S2). The two Pleistocene shells contain no detectable calcite while four of the six Miocene samples show variable amounts (from  $\sim 0.5\%$ – $45\%$ ) of calcite (Table S2). The mid-Pliocene shell samples from the Kunlun Pass Basin had traces ( $\sim 0.5\%$ ) of calcite. Among the Pliocene fossil shells analyzed from the Zanda Basin, 14 out of 24 samples had trace amounts of calcite ( $\sim 0.4\%$  to  $1.2\%$ ). Clumped isotope analyses of a subset of these fossil shell samples yielded a wide range of temperatures (Fig. 5B; Table S3). The  $\Delta_{47}$ -derived temperatures vary from  $-5$  °C to  $21$  °C, with a range of  $26$  °C, using the Henkes calibration and from  $2$  °C to  $25$  °C, with a range of  $23$  °C, using the Eagle calibration. The long-term temperature measurements from 1935 to 1990 at a meteorological station in Lhasa ( $29.67^\circ\text{N}$   $91.10^\circ\text{E}$ , elevation 3600 m) show that the monthly average air temperature varied from  $-1.2$  °C in January to  $16.5$  °C in June, with an annual monthly temperature range of  $18$  °C (<http://www.worldclimate.com>, accessed September 2020). The temperature range in our fossil shells from the Zanda Basin greatly exceeds the modern monthly temperature range recorded in Lhasa as well as the variation range of lake water temperatures observed at a high-elevation lake site in the central Tibetan Plateau (Huntington et al., 2015). This indicates that the clumped isotope signatures of some of the shells may have been altered. As shown in

TABLE 1. TWO-TAILED *T*-TEST RESULTS FOR SIGNIFICANT CLUMPED ISOTOPE TEMPERATURE DIFFERENCES BETWEEN MEAN VALUES OF DIFFERENT SAMPLE GROUPS

	Mean difference	<i>df</i>	<i>t</i>	<i>p</i>	Significant difference at 95%
Pristine fossil shells vs. fossil shells with trace calcite (ZD)	9.8	16	3.71	0.002	Yes
Pristine fossil shells vs. all fossils with trace calcite	10.9	18	4.34	0.0004	Yes
Pristine vs. modern	3.8	37	2.68	0.01	Yes
Fossil shells with trace calcite (ZD) vs. modern	-6.0	35	-3.48	0.001	Yes
All fossil shells with trace calcite vs. modern	-7.1	37	-4.41	<0.0001	Yes

Note: ZD—Zanda Basin. *df*, *t* and *P* are the degree of freedom, *t*-value, and *P*-value, respectively, of the statistical test.

Figure 5B, fossil shells with traces of calcite generally yielded much lower clumped isotope temperatures than pristine fossil shells, indicating that clumped isotope alteration may have occurred in these shells that contain detectable calcite. The average  $\delta^{13}\text{C}$  and  $\delta^{18}\text{O}$  values of fossil shells with trace amounts of calcite are also slightly lower than those of the pristine fossils (Fig. 5C). This may be further evidence for isotopic alteration of these shells. Statistical tests show that the temperature difference between our pristine fossil shells and shells containing trace amounts of calcite is highly significant (Table 1). The clumped isotope temperatures of our pristine fossil shell samples are on average  $\sim 10^\circ\text{C}$  higher than the shells containing traces of calcite from the same strata regardless of the calibration used (Figs. 5B). These observations suggest that clumped isotope ordering in aragonite shells can be readily altered in low-temperature environments and significant alteration can occur even in shells containing only traces of calcite and with no visible signs of recrystallization.

We previously reported clumped isotope temperature data from four mid-Pliocene fossil shells from Tibet (Wang et al., 2013b). Unfortunately, these and other initial samples analyzed at Caltech (Table S3) were selected solely based on visual inspection. Subsequent XRD analyses of these samples reveal that these “well-preserved” samples all had a trace amount of calcite ranging from  $-0.4\%$  to  $0.8\%$  (Table S3), indicating alteration by diagenesis. Thus, the temperatures derived from the  $\Delta_{47}$  values of these four shells do not reflect the original temperatures of shell formation. Similarly, the Pliocene shell samples from the Kunlun Pass Basin had a detectable amount of calcite ( $\sim 0.5\%$ ), indicating that the  $\Delta_{47}$ -derived temperatures from those two samples are also unreliable (Table S3).

Temperatures derived from the  $\Delta_{47}$  values of our pristine Pliocene fossil shells from the Zanda Basin in southwestern Tibet are  $14 \pm 5^\circ\text{C}$  with a range of  $8^\circ\text{C}$  to  $21^\circ\text{C}$  using the Henkes calibration or  $19 \pm 4^\circ\text{C}$ , ranging from  $13^\circ\text{C}$  to  $25^\circ\text{C}$ , using the Eagle calibration (Fig. 5B). In comparison, Pliocene fossil shells with trace amounts of calcite from the Zanda Basin yielded significantly lower  $\Delta_{47}$  temperatures of  $4 \pm 7^\circ\text{C}$  using

the Henkes calibration or  $10 \pm 6^\circ\text{C}$  using the Eagle calibration (Fig. 5B; Table 1). Huntington et al. (2015) reported  $\Delta_{47}$ -derived temperatures from eight fossil shells ranging in age from the late Miocene to the mid Pliocene from the same strata in the Zanda Basin. The average temperatures calculated from the  $\Delta_{47}$  values of their fossil shells are  $6 \pm 3^\circ\text{C}$  (with a range of  $2^\circ\text{C}$  to  $10^\circ\text{C}$ ) using the Henkes calibration and  $11 \pm 3^\circ\text{C}$  (varying from  $8^\circ\text{C}$  to  $16^\circ\text{C}$ ) using the Eagle calibration. These temperatures are lower than the average temperature derived from our pristine Pliocene fossil shells but are very similar to those derived from our fossil shells that contain traces of calcite.

The relatively large temperature range observed in pristine fossil shells may indicate that some of the shells analyzed were not autochthonous but were transported by rivers from high elevations into the lake. However, this interpretation is inconsistent with the lithological evidence. As noted previously, our fossil shells were collected from fine-grained sediments, which suggests a lacustrine origin. The  $\delta^{18}\text{O}$  data from the shells also do not support this interpretation. The  $\delta^{18}\text{O}$  values of pristine fossil shells are generally within the  $\delta^{18}\text{O}$  range of modern shells (Fig. 5C; Tables S1 and S3), suggesting that the fossil snails, like their modern counterpart, lived in an evaporated water body such as a lake. The water  $\delta^{18}\text{O}$  values calculated from the clumped isotope temperatures and  $\delta^{18}\text{O}$  values of pristine fossil shells from Zanda Basin using the equation of Kim et al. (2007) are  $-4 \pm 1\%$  (Table S3), much higher than the  $\delta^{18}\text{O}$  of paleo-meteoric water (i.e.,  $-14 \pm 2\%$  at 4.2 Ma and  $-19 \pm 1\%$  at ca. 3.8 Ma) estimated from the tooth enamel  $\delta^{18}\text{O}$  values of fossil mammals from the basin (Wang et al., 2013b). This provides further evidence indicating that these shells are of lacustrine origin as evaporation preferentially removes isotopically light water molecules leading to higher  $\delta^{18}\text{O}$  values of lake water relative to local precipitation and river water (Gonfiantini, 1986). The temperature variability of our pristine fossil shells is comparable to the observed variability in modern shells from Tibetan lakes (Figs. 2 and 5B), most likely reflecting variations in the size (or lifespan) and formation time of the shells analyzed (Roy et al., 2019).

## Comparison with Modern Shells and Implications for Paleoclimate and Paleoelevation

The clumped isotope temperatures of our modern shells from various lakes on the Tibetan Plateau are significantly lower than those of the pristine fossil shells but higher than those of fossil shells containing trace calcite (Table 1), regardless of which calibration is used. As shown in Figure 6A, the average clumped isotope temperature of modern shells falls at about the midpoint between the MAWT and summer water temperature predicted using the modern relationships between MAAT and elevation for the region (Quade et al., 2011) and between lake water temperatures and MAAT (Hren and Sheldon, 2012). In comparison, the average temperature of pristine fossils is almost the same as the predicted present-day summer water temperature at the sample site while fossil shells with trace calcite yielded an average temperature that is lower than the predicted MAWT but similar to, or slightly higher than, the estimated MAAT for their present-day elevation (Fig. 6A).

Fossil species that we analyzed from the Zanda Basin are thought to have lived in a shallow littoral lake environment (Han et al., 2012). Assuming that these Pliocene freshwater snails had habits similar to those of their modern relatives (Taft et al., 2012; Roy et al., 2019), the difference in clumped isotope temperatures between the pristine fossil shells and modern shells would indicate that the Zanda Basin was warmer in the early and mid-Pliocene (ca. 4–5 Ma) than today (Fig. 6B). Because temperature decreases with increasing elevation, any change in temperature at high elevations in a tectonically active region such as our study area could be caused by either elevation change or global climate change or both (Wang et al., 2012; Wang et al., 2008). The difference in  $\Delta_{47}$ -derived temperatures between the pristine fossil and modern freshwater mollusk shells can be explained by the change in global climate. Paleotemperature reconstructions based on geochemical proxies preserved in marine sediments indicate that the Earth's climate was considerably warmer during the early Pliocene (5.3–3.6 Ma), with higher sea level and less polar ice, than today (e.g., Fedorov et al., 2013; Lear et al., 2000). Climate simulations using global climate models forced with different sea surface temperature reconstructions suggest that the global mean temperature during the early Pliocene warmth was  $\sim 3\text{--}4^\circ\text{C}$  higher than the modern temperature (Brierley and Fedorov, 2010; Haywood and Valdes, 2004). The temperature difference between our pristine fossil and modern shells, after adjusting for temperature change ( $\sim 1\text{--}1.5^\circ\text{C}$ ) due to the sampling elevation difference (Fig. 6A), is



similar to the change in global mean temperature since the Pliocene warm period (Brierley and Fedorov, 2010; Haywood and Valdes, 2004). This suggests that the elevation of the Zanda Basin at ca. 4–5 Ma was similar to its present-day elevation, which is consistent with the mammalian fossil record and enamel isotope data from the basin (Deng et al., 2012; Deng et al., 2011; Wang et al., 2015; Wang et al., 2013b), and the temperature change in the area since ca. 5–4 Ma was most likely the local manifestation of the global climate change.

### Limitations and Future Direction

Our combined XRD and clumped isotope analyses of fossil shells from high-elevation fossil basins on the Himalayan-Tibetan Plateau show that the clumped isotope signatures of aragonite shells can be readily altered in low-temperature environments at or near the Earth's surface, and significant alteration could happen even in shells with no visible signs of recrystallization. Our data suggest that clumped isotope alteration in aragonite shells can occur with <1% of calcite replacement in the shell. The results underscore the importance of screening each “well-preserved” fossil shell sample before conducting much more expensive and time-consuming clumped isotope analysis. All of the fossil shells analyzed in this study appeared to be pristine based on visual inspection and are purely or almost purely aragonite (Fig. 5A; Table S2). However, as seen in our data (Figs. 5B; Table S3), just a trace amount of calcite replacement in an aragonite shell could significantly affect the  $\Delta_{47}$  signature and thus the  $\Delta_{47}$ -derived temperature of the shell. This observation cannot be explained by simple mixing of unaltered aragonite with trace amounts of diagenetic calcite as demonstrated by the isotope mass balance calculations using a simple two component (i.e., diagenetic calcite and pristine aragonite) mixing model (Fig. S2). This suggests that other factors or processes besides micro-scale solution of aragonite and precipitation of calcite have played an important role in altering the clumped isotope signatures of the shells. Below, we explore the possibility that isotopic alteration was caused by solid-state bond reordering.

Both experimental studies and analyses of natural samples have demonstrated that the isotopic compositions of carbonate minerals such as calcite can be readily altered at high temperatures as a result of solid-state diffusion and isotope exchange between adjacent carbonate ions in the crystal lattice (e.g., Chen et al., 2019; Dennis and Schrag, 2010; Farver, 1994; Henkes et al., 2014; Passey and Henkes, 2012; Stolper and Eiler, 2015). Stolper and Eiler (2015) show

that solid state reordering can begin at relatively low temperatures of 80–90 °C. Recently, Staudigel and Swart (2016) conducted a series of heating experiments with aragonite at various temperatures ranging from 125 °C to 425 °C over the course of a few hours up to ~2 weeks. Although none of their samples reached thermodynamic equilibrium, their results show that the clumped isotope composition of aragonite is extremely susceptible to alteration and can quickly change from “initial composition to an apparent equilibrium state with no observed change in mineralogy” at temperatures as low as 125 °C, which they attributed to the result of solid-state isotopic reactions (Staudigel and Swart, 2016). They further suggest that water trapped in the mineral may have lowered the energetic barriers for these reactions as the rates of change were much faster than those for purely solid-state driven processes observed in calcite (Staudigel and Swart, 2016). Similarly, Chen et al. (2019) performed heating experiments with aragonite and calcite at temperatures of 200–500 °C for various durations ranging from ~5 min up to 6 days. Their results confirm the previous findings that the bond reordering in aragonite does not follow the first-order kinetics and occurs faster than in calcite and that the clumped isotope composition of aragonite can be altered even before conversion to calcite (Chen et al., 2019). Although all of the experimental studies were carried out at elevated temperatures for very short periods of time (from minutes up to 2 weeks) and rates of change are expected to be much slower at low temperatures, our new data are consistent with the possibility that clumped isotope compositions of biogenic aragonite can be altered even at near freezing temperatures over geologic time scales (Fig. 5B).

Currently, there are no unequivocally accurate rate constants and kinetic models for clumped isotope reordering in aragonite available in the literature (Chen et al., 2019). Assuming that the solid-state isotope exchange in aragonite approximately follows the first-order kinetics and that the Arrhenius parameters estimated by Staudigel and Swart (2016) based on their experimental results (i.e.,  $E_a = 1.1 \times 10^5$  J/mol and  $\ln(k_0) = 21.7$ ) are applicable to our shells, we estimated the rate constants of solid-state bond reordering and simulated the clumped isotope evolution in aragonite at low temperatures using the Arrhenius equation ( $k = k_0 \cdot e^{-E_a/(RT)}$ , where  $k$  = rate constant,  $E_a$  = activation energy,  $R$  = universal gas constant,  $T$  = temperature) and the Equation (3) in Staudigel and Swart (2016) (Fig. S3). Although these estimates may be unreliable due to insufficient kinetic data and the (likely) oversimplified kinetic model, this simple exercise shows that it is plausible for reordering

to occur in aragonite at Earth-surface temperatures over time scales of only a few hundreds of years and longer (Fig. S3).

An alternative explanation for alteration in  $\Delta_{47}$  is microscale solution-precipitation that preserves aragonite mineralogy but does not result in large shifts in  $\delta^{13}\text{C}$  and  $\delta^{18}\text{O}$  because of low fluid-mineral ratios during the solution-precipitation process. We speculate that annual freeze-thaw cycles in the high-elevation environment on the present-day Tibetan Plateau and decomposition of organic material within biogenic aragonite could have facilitated such a process or possibly also lowered the energetic barriers for solid-state isotopic reordering (or isotope exchange among adjacent carbonate ions) in aragonite.

Regardless of the mechanism(s) for clumped isotope reordering, our findings have important implications for paleoclimate and paleoelevation reconstructions using clumped isotope data from aragonite fossil shells. In future studies, aragonite fossil shell samples for clumped isotope study should all be pre-screened using XRD or other means, especially samples older than the Pleistocene in age, and only the shells with no detectable amounts of calcite should be used for paleotemperature and paleoelevation reconstructions. Further research is needed to examine the mineral phases in fossil shells using multiple tools including, for instance, petrographic microscope, scanning electronic microscope, electron backscatter diffraction, and transmission electron microscope images, in conjunction with XRD analysis. This will help to better understand the nature of the alteration process. Another focus area for future research is to investigate the mechanism of low-temperature clumped isotope reordering in biogenic aragonite through experimental and modeling studies. Efforts are also needed to improve the precision and accuracy of clumped isotope analysis.

### CONCLUSION

Clumped isotope analyses of modern snail shells from several lakes across the Himalayan-Tibetan plateau show that temperatures determined from the shells using the existing mollusk specific calibrations (i.e., the Eagle calibration and the Henkes calibration) differ by ~6 °C. Some of the temperatures calculated using the Eagle calibration exceed the observed and predicted maximum lake water temperature while those calculated using the Henkes calibration all fall within the variation range of lake surface water temperature, suggesting that the Henkes calibration may be more suitable for freshwater snail shells.

Combined XRD and clumped isotope analyses of fossil freshwater snail shells from the

plateau show that clumped isotope signatures of aragonite shells can be readily altered in low-temperature diagenetic environments. More than half of the fossil shells analyzed in this study contain trace amounts of calcite, despite lacking visible signs of recrystallization. The clumped isotope temperatures of our fossil shells with traces of calcite are significantly lower than those of the pristine fossils, suggesting that clumped isotope reordering can occur with just a trace amount of calcite replacement in the shell. Solid-state isotopic reordering, or exchange among adjacent carbonate ions, is plausibly an important process altering the clumped isotope signatures of aragonite shells in low-temperature diagenetic environments, although micro-scale mineral-buffered solution of aragonite and reprecipitation of aragonite and/or calcite could also result in altered clumped isotope compositions. We recommend for future studies that each aragonite fossil shell sample be screened for traces of calcite using XRD or other means, such as electron backscatter diffraction, before performing clumped isotope analysis. Our data also show that the clumped isotope temperatures of pristine fossil shells from the Zanda Basin in southwestern Tibet are on average  $\sim 4$  °C higher than those of the modern shells from high-elevation lakes on the Tibetan plateau, which indicates that the basin was warmer during the early and mid-Pliocene than today. After accounting for temperature change due to global cooling, the difference in  $\Delta_{47}$ -derived temperatures between our pristine fossil shells and modern shells suggests that the paleoelevation of the Zanda Basin 4–5 m.y. ago was similar to its present-day elevation, in agreement with the inference from the carbon isotope data and fossil records from the basin.

#### ACKNOWLEDGMENTS

This study was supported by an award from The Council on Research & Creativity of Florida State University and grants from the Chinese Academy of Sciences (XDB26000000, XDA20070203) and the National Natural Science Foundation of China (41430102 and 41888101). Sample preparation and stable isotope analysis of water samples were performed at the National High Magnetic Field Laboratory, which is supported by National Science Foundation Cooperative Agreement No. DMR-1644779 and the State of Florida. The UCLA mass spectrometry contributions were also supported by Department of Energy Basic Energy Sciences grant DE-FG02-13ER16402, and personnel by National Science Foundation EAR-1352212.

#### REFERENCES CITED

An, Z., Kutzbach, J.E., Prell, W.L., and Porter, S.C., 2001, Evolution of Asian monsoons and phased uplift of the Himalayan Tibetan plateau since Late Miocene times: *Nature*, v. 411, no. 6833, p. 62–66, <https://doi.org/10.1038/35075035>.

- Botsyun, S., Sepulchre, P., Donnadieu, Y., Risi, C., Licht, A., and Rugenstein, J., 2019, Revised paleoaltimetry data show low Tibetan Plateau elevation during the Eocene: *Science*, v. 363, no. eaaq1436, <https://doi.org/10.1126/science.aaq1436>.
- Brierley, C.M., and Fedorov, A.V., 2010, Relative importance of meridional and zonal sea surface temperature gradients for the onset of the ice ages and Pliocene-Pleistocene climate evolution: *Paleoceanography*, v. 25, no. PA2214, <https://doi.org/10.1029/2009PA001809>.
- Chen, S., Ryb, U., Piasecki, A.M., Lloyd, M.K., Baker, M.B., and Eiler, J.M., 2019, Mechanism of solid-state clumped isotope reordering in carbonate minerals from aragonite heating experiments: *Geochimica et Cosmochimica Acta*, v. 258, p. 156–173, <https://doi.org/10.1016/j.gca.2019.05.018>.
- DeCelles, P.G., Quade, J., Kapp, P., Fan, M.J., Dettman, D.L., and Ding, L., 2007, High and dry in central Tibet during the Late Oligocene: *Earth and Planetary Science Letters*, v. 253, no. 3–4, p. 389–401, <https://doi.org/10.1016/j.epsl.2006.11.001>.
- Deng, T., and Ding, L., 2015, Paleo-altimetry reconstructions of the Tibetan Plateau: Progress and contradictions: *National Science Review*, v. 2, p. 417–437, <https://doi.org/10.1093/nsr/nwv062>.
- Deng, T., Wang, X.M., Fortelius, M., Li, Q., Wang, Y., Tseng, Z.J., Takeuchi, G.T., Saylor, J.E., Saita, L.K., and Xie, G.P., 2011, Out of Tibet: Pliocene woolly rhino suggests high-plateau origin of Ice Age megaherbivores: *Science*, v. 333, no. 6047, p. 1285–1288, <https://doi.org/10.1126/science.1206594>.
- Deng, T., Li, Q., Tseng, Z.J., Takeuchi, G.T., Wang, Y., Xie, G.P., Wang, S.Q., Hou, S.K., and Wang, X.M., 2012, Locomotive implication of a Pliocene three-toed horse skeleton from Tibet and its paleo-altimetry significance: *Proceedings of the National Academy of Sciences of the United States of America*, v. 109, no. 19, p. 7374–7378, <https://doi.org/10.1073/pnas.1201052109>.
- Deng, T., Wang, X., Wu, F., Wang, Y., Li, Q., Wang, S., and Hou, S., 2019, Review: Implications of vertebrate fossils for paleo-elevations of the Tibetan Plateau: *Global and Planetary Change*, v. 174, p. 58–69, <https://doi.org/10.1016/j.gloplacha.2019.01.005>.
- Dennis, K., and Schrag, D., 2010, Clumped isotope thermometry of carbonatites as an indicator of diagenetic alteration: *Geochimica et Cosmochimica Acta*, v. 74, p. 4110–4122, <https://doi.org/10.1016/j.gca.2010.04.005>.
- Dennis, K.J., Affek, H.P., Passey, B.H., Schrag, D.P., and Eiler, J.M., 2011, Defining an absolute reference frame for ‘clumped’ isotope studies of CO<sub>2</sub>: *Geochimica et Cosmochimica Acta*, v. 75, p. 7117–7131, <https://doi.org/10.1016/j.gca.2011.09.025>.
- Eagle, R.A., Eiler, J.M., Tripathi, A.K., Ries, J.B., Freitas, P.S., Hiebenthal, C., Wanamaker, A.D., Taviani, M., Elliot, M., Marensi, S., Nakamura, K., Ramirez, P., and Roy, K., 2013, The influence of temperature and seawater carbonate saturation state on <sup>13</sup>C-<sup>18</sup>O bond ordering in bivalve mollusks: *Biogeosciences*, v. 10, no. 7, p. 4591–4606, <https://doi.org/10.5194/bg-10-4591-2013>.
- Eiler, J., 2011, Paleoclimate reconstruction using carbonate clumped isotope thermometry: *Quaternary Science Reviews*, v. 30, p. 3575–3588, <https://doi.org/10.1016/j.quascirev.2011.09.001>.
- Farver, J.R., 1994, Oxygen self-diffusion in calcite: Dependence on temperature and water fugacity: *Earth and Planetary Science Letters*, v. 121, p. 575–587, [https://doi.org/10.1016/0012-821X\(94\)90092-2](https://doi.org/10.1016/0012-821X(94)90092-2).
- Fedorov, A.V., Brierley, C.M., Lawrence, K.T., Liu, Z., Dekens, P.S., and Ravelo, A.C., 2013, Patterns and mechanisms of early Pliocene warmth: *Nature*, v. 496, no. 7443, p. 43, <https://doi.org/10.1038/nature12003>.
- Ghosh, P., Adkins, J., Affek, H., Balta, B., Guo, W.F., Schauble, E.A., Schrag, D., and Eiler, J.M., 2006a, <sup>13</sup>C-<sup>18</sup>O bonds in carbonate minerals: A new kind of paleothermometer: *Geochimica et Cosmochimica Acta*, v. 70, no. 6, p. 1439–1456, <https://doi.org/10.1016/j.gca.2005.11.014>.
- Ghosh, P., Garzzone, C.N., and Eiler, J.M., 2006b, Rapid uplift of the Altiplano revealed through <sup>13</sup>C-<sup>18</sup>O bonds in paleosol carbonates: *Science*, v. 311, no. 5760, p. 511–515, <https://doi.org/10.1126/science.1119365>.
- Gonfiantini, R., 1986, Environmental isotopes in lake studies, in Fontes, F.P., *Handbook of Environmental Isotope Geochemistry: The Terrestrial Environment*, Volume 2: New York, Elsevier Science Publishing Co., p. 113–168.
- Han, J., Yu, J., He, C., Meng, Q., Zhu, D., Meng, X., Shao, Z., and Yang, C., 2012, The assemblage of gastropod fossils in Zanda Basin of Tibet and its biostratigraphy: *Acta Geoscientia Sinica*, v. 33, no. 2, p. 153–166.
- Haywood, A.M., and Valdes, P.J., 2004, Modelling Pliocene warmth: Contribution of atmosphere, oceans and cryosphere: *Earth and Planetary Science Letters*, v. 218, no. 3–4, p. 363–377, [https://doi.org/10.1016/S0012-821X\(03\)00685-X](https://doi.org/10.1016/S0012-821X(03)00685-X).
- Henkes, G.A., Passey, B.H., Wanamaker, A.D., Grossman, E.L., Ambrose, W.G., and Carroll, M.L., 2013, Carbonate clumped isotope compositions of modern marine mollusk and brachiopod shells: *Geochimica et Cosmochimica Acta*, v. 106, p. 307–325, <https://doi.org/10.1016/j.gca.2012.12.020>.
- Henkes, G.A., Passey, B.H., Grossman, E.L., Shenton, B.J., Perez-Huerta, A., and Yancey, T.E., 2014, Temperature limits for preservation of primary calcite clumped isotope paleotemperatures: *Geochimica et Cosmochimica Acta*, v. 139, p. 362–382, <https://doi.org/10.1016/j.gca.2014.04.040>.
- Hren, M.T., and Sheldon, N.D., 2012, Temporal variations in lake water temperature: Paleoenvironmental implications of lake carbonate  $\delta^{18}\text{O}$  and temperature records: *Earth and Planetary Science Letters*, v. 337, p. 77–84, <https://doi.org/10.1016/j.epsl.2012.05.019>.
- Huntington, K.W., Eiler, J.M., Affek, H.P., Guo, W., Bonifacie, M., Yeung, L.Y., Thiagarajan, N., Passey, B., Tripathi, A., Daeron, M., and Came, R., 2009, Methods and limitations of ‘clumped’ CO<sub>2</sub> isotope ( $\Delta_{47}$ ) analysis by gas-source isotope ratio mass spectrometry: *Journal of Mass Spectrometry*, v. 44, no. 9, p. 1318–1329, <https://doi.org/10.1002/jms.1614>.
- Huntington, K.W., Saylor, J., Quade, J., and Hudson, A.M., 2015, High late Miocene–Pliocene elevation of the Zhada Basin, southwestern Tibetan Plateau, from carbonate clumped isotope thermometry: *Geological Society of America Bulletin*, v. 127, p. 181–199, <https://doi.org/10.1130/B31000.1>.
- Kim, S.T., O’Neil, J.R., Hillaire-Marcel, C., and Mucci, A., 2007, Oxygen isotope fractionation between synthetic aragonite and water: Influence of temperature and Mg<sup>2+</sup> concentration: *Geochimica et Cosmochimica Acta*, v. 71, p. 4704–4715, <https://doi.org/10.1016/j.gca.2007.04.019>.
- Lear, C.H., Elderfield, H., and Wilson, P.A., 2000, Cenozoic deep-sea temperatures and global ice volumes from Mg/Ca in benthic foraminiferal calcite: *Science*, v. 287, no. 5451, p. 269–272, <https://doi.org/10.1126/science.287.5451.269>.
- Li, J., and Zhou, Y., 2002, Palaeovegetation type analysis of the late Pliocene in Zanda Basin of Tibet: *Journal of Palaeogeography*, v. 4, p. 52–58.
- Li, Q., Xie, G.P., Takeuchi, G.T., Deng, T., Tseng, Z.J., Grohé, C., and Wang, X., 2014, Vertebrate fossils on the roof of the world: Biostratigraphy and geochronology of high elevation Kunlun Pass Basin, northern Tibetan Plateau, and basin history as related to the Kunlun strike-slip fault: *Palaeogeography, Palaeoclimatology, Palaeoecology*, v. 411, p. 46–55, <https://doi.org/10.1016/j.palaeo.2014.06.029>.
- Meng, X., Zhu, D., Shao, Z., Yang, C., Sun, L., Wang, J., Han, T., Du, J., Han, J., and Yu, J., 2004, Discovery of rhinoceros fossils in the Pliocene in the Zanda Basin, Ngari area, Tibet: *Geological Bulletin of China*, v. 23, p. 609–612.
- Mischke, S., Sun, Z.C., Hertzschuh, U., Qiao, Z.Z., and Sun, N., 2010, An ostracod-inferred large Middle Pleistocene freshwater lake in the presently hyper-arid Qaidam Basin (NW China): *Quaternary International*, v. 218, no. 1–2, p. 74–85, <https://doi.org/10.1016/j.quaint.2009.03.002>.
- Molnar, P., Houseman, G., and England, P., 2006, Paleoaltimetry of Tibet: *Nature*, v. 444, no. E4, <https://doi.org/10.1038/nature05368>.
- Murphy, M.A., Saylor, J.E., and Ding, L., 2009, Late Miocene topographic inversion in southwest Tibet based on integrated paleoelevation reconstructions and structural history: *Earth and Planetary Science Letters*, v. 282, no. 1–4, p. 1–9, <https://doi.org/10.1016/j.epsl.2009.01.006>.

- Økland, J., 1990, Lakes and snails., in Backhuys, D.W., ed., *Environment and Gastropoda in 1,500 Norwegian Lakes, Ponds and Rivers.*: Oegstgeest, The Netherlands, Universal Book Services, p. 516.
- Passey, B.H., and Henkes, G.A., 2012, Carbonate clumped isotope bond reordering and geospeedometry: Earth and Planetary Science Letters, v. 351, p. 223–236, <https://doi.org/10.1016/j.epsl.2012.07.021>.
- Passey, B.H., Levin, N.E., Cerling, T.E., Brown, F.H., and Eiler, J.M., 2010, High-temperature environments of human evolution in East Africa based on bond ordering in paleosol carbonates: Proceedings of the National Academy of Sciences of the United States of America, v. 107, no. 25, p. 11245–11249, <https://doi.org/10.1073/pnas.1001824107>.
- Petersen, S.V., Deffliese, W.F., Saenger, C., Daëron, M., Huntington, K.W., John, C.M., Kelson, J.R., Bernasconi, S.M., Coleman, A.S., Kluge, T., Olack, G.A., Schauer, A.J., Bajnai, D., Bonifacie, M., Breitenbach, S.F.M., Fiebig, J., Fernandez, A.B., Henkes, G.A., Hodell, D., Katz, A., Kele, S., Lohmann, K.C., Passey, B.H., Peral, M.Y., Petrizzo, D.A., Rosenheim, B.E., Tripathi, A., Venturilli, R., Young, E.D., and Winkelstern, I.Z., 2019, Effects of improved <sup>17</sup>O correction on inter-laboratory agreement in clumped isotope calibrations, estimates of mineral-specific offsets, and temperature dependence of acid digestion fractionation: *Geochemistry, Geophysics, Geosystems*, v. 20, p. 3495–3519.
- Quade, J., Breecker, D.O., Daeron, M., and Eiler, J., 2011, The Paleoclimatology of Tibet: An Isotopic Perspective: *American Journal of Science*, v. 311, no. 2, p. 77–115, <https://doi.org/10.2475/02.2011.01>.
- Quade, J., Eiler, J., Daeron, M., and Achyuthan, H., 2013, The clumped isotope geothermometer in soil and paleosol carbonate: *Geochimica et Cosmochimica Acta*, v. 105, p. 92–107, <https://doi.org/10.1016/j.gca.2012.11.031>.
- Roy, R., Wang, Y., and Jiang, S., 2019, Growth pattern and oxygen isotopic systematics of modern freshwater mollusks along an elevation transect: Implications for paleoclimate reconstruction: *Palaeogeography, Palaeoclimatology, Palaeoecology*, v. 532, no. 109243, <https://doi.org/10.1016/j.palaeo.2019.109243>.
- Ruddiman, W.F., Raymo, M.E., Prell, W., and Kutzbach, J.E., 1997, The uplift-climate connection: A synthesis, in Ruddiman, W.F., ed., *Tectonic uplift and climate change*: New York, Plenum Press, p. 471–515, [https://doi.org/10.1007/978-1-4615-5935-1\\_20](https://doi.org/10.1007/978-1-4615-5935-1_20).
- Saylor, J., Quade, J., Dettman, D., DeCelles, P., Kapp, P., and Ding, L., 2009, The late Miocene through present paleoelevation history of southwestern Tibet: *American Journal of Science*, v. 309, p. 1–42, <https://doi.org/10.2475/01.2009.01>.
- Saylor, J., DeCelles, P., and Quade, J., 2010, Climate-driven environmental change in the Zhada Basin, southwestern Tibetan Plateau: *Geosphere*, v. 6, no. 2, p. 74–92, <https://doi.org/10.1130/GES00507.1>.
- Saylor, J.E., Casturi, L., Shanahan, T.M., Nie, J.S., and Saadeh, C.M., 2016, Tectonic and climate controls on Neogene environmental change in the Zhada Basin, southwestern Tibetan Plateau: *Geology*, v. 44, no. 11, p. 919–922, <https://doi.org/10.1130/G38173.1>.
- Sharp, Z., 2007, *Principles of Stable Isotope Geochemistry*: Upper Saddle River, New Jersey, Pearson Prentice Hall, 343 p.
- Song, C., Gao, D., Fang, X., Cui, Z., Li, J., Yang, S., Jin, H., Burbank, D., and Kirschvink, J., 2005, Late Cenozoic high-resolution magnetostratigraphy in the Kunlun Pass Basin and its implications for the uplift of the northern Tibetan Plateau: *Chinese Science Bulletin*, v. 50, p. 1912–1922, <https://doi.org/10.1360/03wd0314>.
- Staudigel, P.T., and Swart, P.K., 2016, Isotopic behavior during the aragonite-calcite transition: Implications for sample preparation and proxy interpretation: *Chemical Geology*, v. 442, p. 130–138, <https://doi.org/10.1016/j.chemgeo.2016.09.013>.
- Stolper, D.A., and Eiler, J.M., 2015, The kinetics of solid-state isotope-exchange reactions for clumped isotopes: A study of inorganic calcites and apatites from natural and experimental samples: *American Journal of Science*, v. 315, no. 5, p. 363–411, <https://doi.org/10.2475/05.2015.01>.
- Taft, L., Wiechert, U., Riedel, F., Weynell, M., and Zhang, H.C., 2012, Sub-seasonal oxygen and carbon isotope variations in shells of modern *Radix* sp (Gastropoda) from the Tibetan Plateau: Potential of a new archive for palaeoclimatic studies: *Quaternary Science Reviews*, v. 34, p. 44–56, <https://doi.org/10.1016/j.quasirev.2011.12.006>.
- Taft, L., Wiechert, U., Zhang, H., Lei, G., Mischke, S., Plessen, B., Weynell, M., Winkler, A., and Riedel, F., 2013, Oxygen and carbon isotope patterns archived in shells of the aquatic gastropod *Radix*: Hydrologic and climatic signals across the Tibetan Plateau in sub-monthly resolution: *Quaternary International*, v. 290–291, p. 282–298, <https://doi.org/10.1016/j.quaint.2012.10.031>.
- Wang, X., Wang, Y., Li, Q., Tseng, Z., Takeuchi, G., Deng, T., Xie, G., Chang, M., and Wang, N., 2015, Cenozoic vertebrate evolution and paleoenvironment in Tibetan Plateau: Progress and prospects: *Gondwana Research*, v. 27, p. 1335–1354, <https://doi.org/10.1016/j.gr.2014.10.014>.
- Wang, X., Jukar, A.M., Tseng, Z.J., and Li, Q., 2020, Dragon bones from the heavens: European explorations and early palaeontology in Zanda Basin of Tibet, retracing type locality of *Qurliqnorina hundesiensis* and Hippa-
- rion (*Plesiohipparion*) zandaense: *Historical Biology*, <https://doi.org/10.1080/08912963.2020.1777551>.
- Wang, X.M., Li, Q., Xie, G., Saylor, J., Tseng, Z.J., Takeuchi, G., Deng, T., Wang, Y., Hou, S., Liu, J., Zhang, C., Wang, N., and Wu, F., 2013a, Mio-Pleistocene Zanda Basin biostratigraphy and geochronology, pre-Ice Age fauna, and mammalian evolution in western Himalaya: *Palaeogeography, Palaeoclimatology, Palaeoecology*, v. 374, p. 81–95, <https://doi.org/10.1016/j.palaeo.2013.01.007>.
- Wang, Y., Deng, T., and Biasatti, D., 2006, Ancient diets indicate significant uplift of southern Tibet after ca. 7 Ma: *Geology*, v. 34, no. 4, p. 309–312, <https://doi.org/10.1130/G22254.1>.
- Wang, Y., Wang, X.M., Xu, Y.F., Zhang, C.F., Li, Q., Tseng, Z.J., Takeuchi, G., and Deng, T., 2008, Stable isotopes in fossil mammals, fish and shells from Kunlun Pass Basin, Tibetan Plateau: Paleo-climatic and paleo-elevation implications: *Earth and Planetary Science Letters*, v. 270, no. 1–2, p. 73–85, <https://doi.org/10.1016/j.epsl.2008.03.006>.
- Wang, Y., Deng, T., Flynn, L., Wang, X., An, Y., Xu, Y., Parker, W., Lochner, E., Zhang, C., and Biasatti, D., 2012, Late Neogene environmental changes in the central Himalaya related to tectonic uplift and orbital forcing: *Journal of Asian Earth Sciences, Special Issue on Asian Climate and Tectonics*, v. 44, p. 62–76, <https://doi.org/10.1016/j.jseaeas.2011.05.020>.
- Wang, Y., Xu, Y., Khawaja, S., Passey, B., Zhang, C., Wang, X., Li, Q., Tseng, Z., Takeuchi, G., Deng, T., and Xie, G., 2013b, Diet and environment of a mid-Pliocene fauna from southwestern Himalaya: Paleo-elevation implications: *Earth and Planetary Science Letters*, v. 376, p. 43–53, <https://doi.org/10.1016/j.epsl.2013.06.014>.
- Zhang, C., Wang, Y., Li, Q., Wang, X., Deng, T., Tseng, Z., Takeuchi, G., Xie, G., and Xu, Y., 2012, Diets and environments of late Cenozoic mammals in the Qaidam Basin, Tibetan Plateau: Evidence from stable isotopes: *Earth and Planetary Science Letters*, v. 333–334, p. 70–82, <https://doi.org/10.1016/j.epsl.2012.04.013>.
- Zhu, D., Meng, X., Shoa, Z., Yang, C., Han, J., Yu, J., Meng, Q., and Lu, R., 2007, Evolution of the paleovegetation, paleoenvironment and paleoclimate during Pliocene-early Pleistocene in Zhada Basin, Ali, Tibet: *Acta Geologica Sinica*, v. 81, p. 295–306.

SCIENCE EDITOR: ROB STRACHAN  
ASSOCIATE EDITOR: GANQING JIANG

MANUSCRIPT RECEIVED 9 JUNE 2020  
REVISED MANUSCRIPT RECEIVED 10 SEPTEMBER 2020  
MANUSCRIPT ACCEPTED 22 SEPTEMBER 2020

Printed in the USA